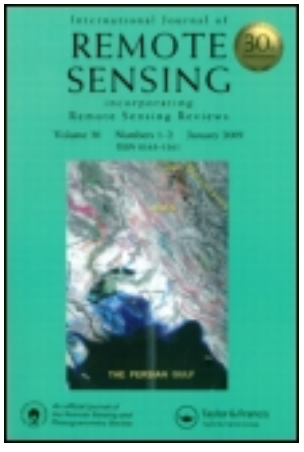

International Journal of Remote Sensing

Publication details, including instructions for authors and subscription information:
http://www.tandfonline.com/loi/tres20

Dependence of mean square slope on wave state and its application in altimeter wind speed retrieval

Shuiqing Li [a], Dongliang Zhao [a], Liangming Zhou [a] & Bin Liu [b]

[a] Physical Oceanography Laboratory, Ocean University of China, Qingdao, 266003, China

[b] Department of Marine, Earth and Atmospheric Sciences, North Carolina State University, Raleigh, NC, 27695, USA

Version of record first published: 10 Sep 2012.

To cite this article: Shuiqing Li, Dongliang Zhao, Liangming Zhou & Bin Liu (2013): Dependence of mean square slope on wave state and its application in altimeter wind speed retrieval, International Journal of Remote Sensing, 34:1, 264-275

To link to this article: http://dx.doi.org/10.1080/01431161.2012.713144

International Journal of Remote Sensing
Vol. 34, No. 1, 10 January 2013, 264–275

Taylor & Francis
Taylor & Francis Group

Dependence of mean square slope on wave state and its application in altimeter wind speed retrieval

Shuiqing Li[a]*, Dongliang Zhao[a], Liangming Zhou[a], and Bin Liu[b]

[a]*Physical Oceanography Laboratory, Ocean University of China, Qingdao 266003, China;*
[b]*Department of Marine, Earth and Atmospheric Sciences, North Carolina State University, Raleigh, NC 27695, USA*

(*Received 29 March 2011; accepted 14 December 2011*)

Mean square slope (MSS) of sea surface is a parameter describing the sea surface roughness and plays a key role in understanding the sea surface dynamics. Although MSS is influenced by many factors such as wind speed and sea surface waves, it has been traditionally parameterized by wind speed only. In this study, the surface wave impact on MSS is investigated using a collocated data set of altimeter and buoy measurements. It is found that the MSS detected by Ku-band altimeter is closely related to the wind wave components and increases with the degree of wind wave development; however, it is almost independent of the swell. The wave effect on MSS is mainly ascribed to the contribution of longer waves rather than shorter waves. An analytical spectral MSS model is proposed, and it is shown that the MSS calculated from the model agrees well with the altimeter-measured MSS when the pseudo-wave age is adjusted to the wave age corresponding to wind waves. This model is applied to derive wind speeds from altimeter data including the normalized radar cross section and the significant wave height of sea surface waves. With the collocated data set, it is shown that this new algorithm performs better than previous empirical algorithms.

1. Introduction

The mean square slope (MSS) of sea surface is defined as the variance of surface slope, which is a key parameter in understanding the air–sea interactions and ocean remote sensing. Air–sea fluxes of mass, momentum, and heat as well as radar scattering are believed to be significantly correlated with MSS. Many factors including wind speed, wave state, air–sea temperature difference, and intensity of sea surfactant films have impacts on the MSS. Since the pioneer work of Cox and Munk (1954), many studies have suggested that the wind speed, which is associated with the short wind waves, dominates the MSS (Jackson et al. 1992; Walsh et al. 1998; Vandemark et al. 2004; Hauser et al. 2009). In addition to wind speed, it has also been shown that the wave state plays an important role in the MSS due to the tilting effect of long waves. However, this effect still remains ambiguous, both qualitatively and quantitatively. In the case of wind waves, Vandemark et al. (2004) found that long-wave (wavelength larger than 2 m) slope variance increases as fetch increases and is largely responsible for the variation of MSS at a given wind speed. It is well known that long waves in the ocean are commonly composed of swells and wind waves. Considering

*Corresponding author. Email: lshq160@gmail.com

ISSN 0143-1161 print/ISSN 1366-5901 online

http://dx.doi.org/10.1080/01431161.2012.713144
http://www.tandfonline.com

the different dynamics between them and their distinct features, it is necessary to take into account their contributions to MSS separately.

According to the quasi-specular theory, the normalized radar cross section (NRCS) measured by altimeter is inversely proportional to the MSS, so it can be regarded as a function of wind speed. In application, researchers usually correlate NRCS with the wind speed directly and have proposed many empirical algorithms for wind retrieval for decades (Chen et al. 2002). Compared with *in situ* measurements, it is shown that the scatter of wind speeds can be improved if the wave state effect is properly considered in the algorithms (Glazman and Greysukh 1993; Lefevre, Barckicke, and Menard 1994; Gourrion et al. 2002; Zhao and Toba 2003; Cheng et al. 2008).

In this article, the wave state effect on the MSS is investigated using a large collocated data set of altimeter and buoy measurements. An analytical MSS model based on wind wave spectrum is developed and validated by the observations. Based on this model, a retrieval algorithm of altimeter wind speed that depends on the NRCS and significant wave height (SWH) is proposed.

2. Collocated data set

The TOPEX/POSEIDON (T/P) altimeter provides the global oceanographic parameters including NRCS, which is related to the sea surface roughness (i.e. MSS). Generally, a lower NRCS value corresponds to a rougher sea surface. The *in situ* observations used in this study are obtained from moored buoys operated by the US National Data Buoy Center (NDBC). To exclude the coastal sheltering and shallow water effects, only the buoys located in deep water and at least 200 km from the land are chosen. A total of 19 NDBC buoys are selected and their locations are shown in Figure 1. Some of the buoys measure the winds at a height of 5 m, and these winds are converted to the winds at 10 m by multiplying by a factor of 1.07, which is determined by the drag coefficient proposed by Wu (1988).

Wind speeds and SWHs measured by buoys, as well as the sea surface roughness in terms of MSS derived from the NRCS of altimeter, can be considered as true observation of the ocean. Therefore, a collocated data set of altimeter and buoy measurements will provide a useful way to analyse the dependence of MSS on the wind speed and SWH.

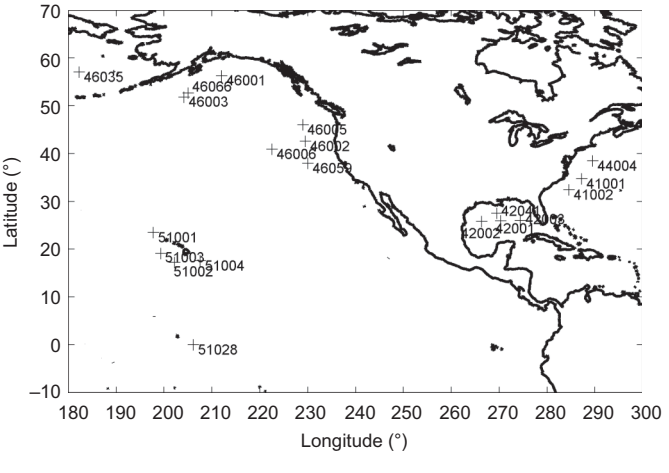

Figure 1. Locations of the 19 NDBC buoys used in the collocated data set.

T/P parameters were extracted when the satellite footprint was within 100 km of the buoy locations and the time difference between the satellite pass and the buoy was less than 30 min. Erroneous altimeter estimates are discarded using conventional data quality flagging suggested by Glazman and Pilorz (1990). The data set has a total of 2623 groups ranging from January 2003 to August 2005.

3. Wave effect on the MSS

At incidence angles less than 150°, the microwave backscattering is primarily due to quasi-specular reflection (Barrick 1974; Holliday, St-Cyr, and Woods 1986; Brown 1990). For an isotropic rough surface of Gaussian distribution, the NRCS due to specular reflection can be expressed as (Valenzuela 1978)

$$\sigma_0 = \left(\frac{|R(0)|^2}{s^2}\right)\left(\sec^4\theta\right)\exp\left[\frac{-\tan^2\theta}{s^2}\right], \tag{1}$$

where σ_0 is the NRCS in natural units, s^2 is the effective MSS, $|R(0)|^2$ is an effective nadir reflection coefficient characterizing the surface reflectivity, and θ is the radar incidence angle.

For an altimeter, $\theta \approx 0°$, and Equation (1) is simplified to

$$\sigma_0 = \frac{|R(0)|^2}{s^2}. \tag{2}$$

It is obvious that the MSS can be determined from NRCS based on Equation (2) if $|R(0)|^2$ is known. In previous studies, $|R(0)|^2$ has been regarded as a constant (Jackson et al. 1992; Wu 1992; Apel 1994; Zhao and Toba 2003; Vandemark et al. 2004; Frew et al. 2007), although the value varies in the range of 0.340−0.427 for the Ku-band of T/P (Table 1).

Recently, Freilich and Vanhoff (2003) showed the dependence of $|R(0)|^2$ on wind speed in their Figure 6, in which $|R(0)|^2$ decreases with wind speed when the wind speed is greater than 3.5 m s^{-1}. This phenomenon can be ascribed to the reduction effect of microwave reflection due to the occurrence of whitecaps (Zheng et al. 1983) and the refraction effect by the short wind waves (Jackson et al. 1992). Both effects increase with increasing wind speed, leading to an overall decrease of $|R(0)|^2$. On the other hand, Freilich and Vanhoff (2003) also found that $|R(0)|^2$ increases with wind speed for speeds less than 3.5 m s^{-1}, and they suggested that this might be a result from the incorrect underestimation of winds by the microwave imager. This part of their data will be excluded in the following discussion.

Table 1. $|R(0)|^2$ for Ku-band of T/P proposed by different authors.

Authors	$\lvert R(0)\rvert^2$
Wu (1992)	0.38
Jackson et al. (1992)	0.38
Apel (1994)	0.34
Zhao and Toba (2003)	0.38
Vandemark et al. (2004)	0.34
Frew et al. (2007)	0.427

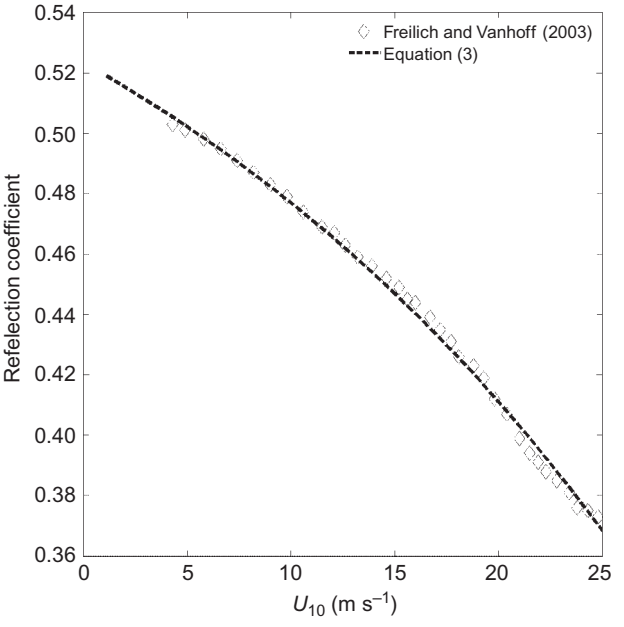

Figure 2. Reflection coefficient of PR versus wind speed. The diamond symbols represent the results of Freilich and Vanhoff (2003), and the dashed curve represents the fitted relationship by Equation (3).

Based on the work of Freilich and Vanhoff (2003), the formula of $|R(0)|^2$ as a function of wind speed for the precipitation radar (PR) with the least square method (Figure 2) is

$$|R(0)|^2_{\mathrm{PR}} = -0.11 \exp\,(0.035U_{10}) + 0.6335, \tag{3}$$

where U_{10} is the wind speed at a height of 10 m and $|R(0)|^2_{\mathrm{PR}}$ is the reflection coefficient corresponding to the PR. This formula is directly extrapolated to wind speed less than 3.5 m s^{-1}.

Tran et al. (2005) reported that there is a systematic offset of NRCS (about 1.29 dB) between PR and T/P, which is independent of wind and wave state. Since the work frequencies of PR (13.8 GHz) and T/P (13.6 GHz) are very close to each other, it seems reasonable to assume that both of them detect almost the same MSS, i.e. $s^2_{\mathrm{TP}} \approx s^2_{\mathrm{PR}}$. So Equation (3) can be converted into

$$|R(0)|^2_{\mathrm{TP}} = -0.08 \exp\,(0.035U_{10}) + 0.47. \tag{4}$$

The values of $|R(0)|^2_{\mathrm{TP}}$ vary between 0.28 and 0.41 for wind speeds in the range of 0−25 m s^{-1}, which generally include the values listed in Table 1.

Using $|R(0)|^2$ expressed in Equation (4), the MSS can be obtained through Equation (2). Figure 3 shows the MSS versus wind speed derived from buoy measurements of the collocated data set; the formulae of MSS for a clean water surface (Wu 1990) and for a sea surface covered by a dense artificial slick (Phillips 1977) are also illustrated as a reference. It can be seen from Figure 3 that most of the T/P MSS values fall into intermediate values between the two formulae, especially for wind speeds higher than 5 m s^{-1}. This is

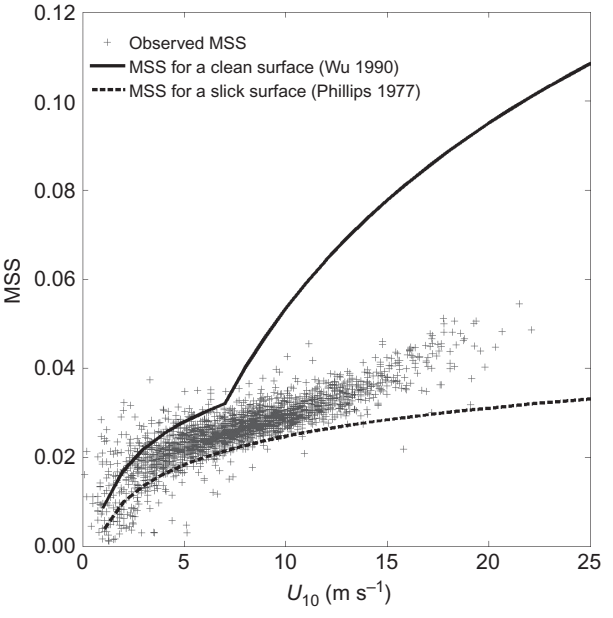

Figure 3. MSS as a function of wind speed.

because the MSS from a clean surface measured by the optical method is believed to be the upper limit, and the result from a slick surface can be regarded as the lower limit since the contribution of short waves is excluded. However, at the same time, the scatter of the MSS indicates that other factors except wind speed affect the MSS. Many studies have shown that the most important candidates are the ocean waves including wind waves and swells (Zhao and Toba 2003; Vandemark et al. 2004).

The wave state can be denoted by the wave age, which is traditionally defined as the ratio of the phase speed corresponding to the spectral peak to the wind speed U_{10}. In deep water, it is expressed as the following:

$$\beta = \frac{gT_{\mathrm{p}}}{2\pi U_{10}}, \tag{5}$$

where T_{p} is the period corresponding to the spectral peak and g is the acceleration due to gravity. For the altimeter, the wave period is unknown, so a parameter called pseudo-wave age (β'), proposed by Glazman and Pilorz (1990), has been used to characterize the wave state, which is defined by the SWH, H_{s}, and wind speed:

$$\beta' = 3.24\left(\frac{gH_s}{U_{10}^2}\right)^{0.62}. \tag{6}$$

Figure 4 illustrates the bin-averaged MSS at the given wind speed range versus β and β', respectively. It can be seen that the MSS increases with both β and β' at smaller wave ages in general. This trend becomes obscure at larger wave ages. The MSS correlated better with β' than with β. The enhancement of MSS with the wave age can also be seen from Figure 5,

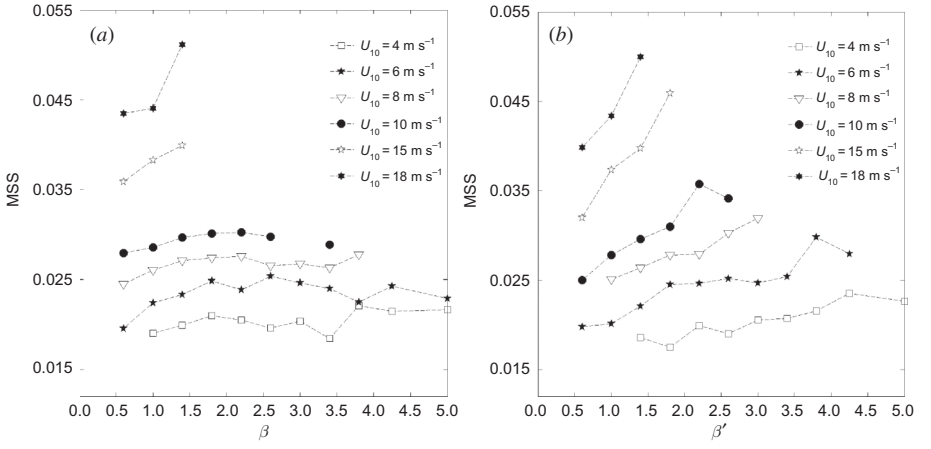

Figure 4. Bin-averaged MSS versus wave ages β (*a*) and β' (*b*) at given wind speed ranges.

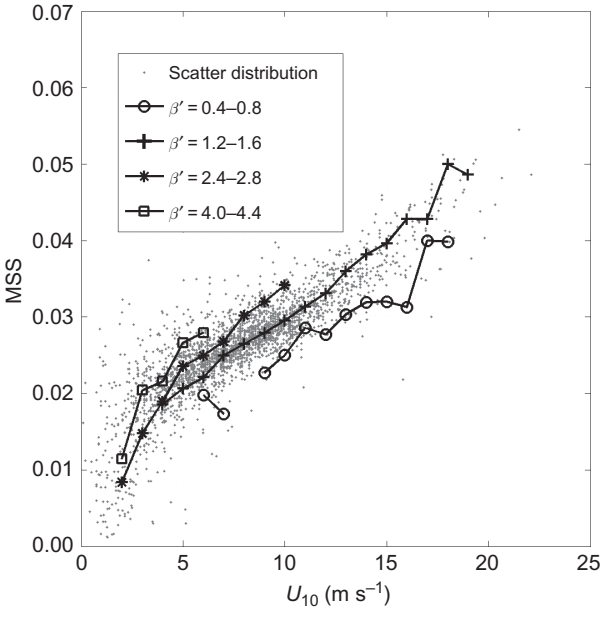

Figure 5. MSS versus wind speed. The data are divided into four groups according to the wave age β', and the MSS is averaged within wind speed bins of 1 m s^{-1}.

in which the wave ages are divided into four groups. At a given wind speed, MSS increases roughly with the wave age β'.

In principle, the NRCS or MSS should closely correlate with wind waves, which are directly forced by winds. Some studies found that the longer waves corresponding to swells have little effect on the NRCS (Nghiem et al. 1995). Therefore, the contributions to MSS from swells should be separated from those by wind waves. Based on the method proposed by Earle (1984) and the buoy data from the collocated data set, the total SWH can be partitioned into two parts, which correspond to wind waves and swells. It is found that the

MSS increases with the increasing SWH of wind waves, with a correlation coefficient of 0.84, and that the MSS is almost independent of the SWH of swells, with a correlation coefficient of −0.06. Thus, the wave effect on the MSS or NRCS is mainly ascribed to the contribution of wind waves.

4. Spectral approach

Another method to obtain the MSS is the integration of wave spectrum, which is defined as (Phillips 1977)

$$s^2 = \int_0^\infty \boldsymbol{k}^2 \varphi\left(\vec{\boldsymbol{k}}\right) \mathrm{d}\vec{\boldsymbol{k}}, \tag{7}$$

where $\varphi(\vec{\boldsymbol{k}})$ is the wavenumber spectrum of ocean waves and $\vec{\boldsymbol{k}}$ is the wavenumber vector. With the dispersion relationship of surface wave, Equation (7) can be transformed into the integration of the frequency spectrum of the surface wave, $F(f)$, which is usually measured by the buoy. For gravity waves, it can be rewritten as

$$s^2 = \int_0^\infty \frac{(2\pi f)^4}{g^2} F(f)\mathrm{d}f, \tag{8}$$

where f is the frequency. As for the NDBC buoys, the cut-off frequencies are in the range of 0.4–0.5 Hz. Thus, the calculated MSS from wave spectra measured by these buoys can be considered as the MSS for long waves. Subtracting it from the MSS detected by altimeter mentioned above, the residual is supposed to be the MSS for short waves.

Figure 6 shows the MSS versus wind speed for long and short waves. It is averaged in bins of U_{10} at different β' ranges. It can be seen that the MSS for long waves increases as the wave age increases, and the MSS for short waves is independent of wave age. The magnitude of the former is significantly smaller than that of the latter, which suggests that the short ocean waves play a more important role in the sea surface roughness.

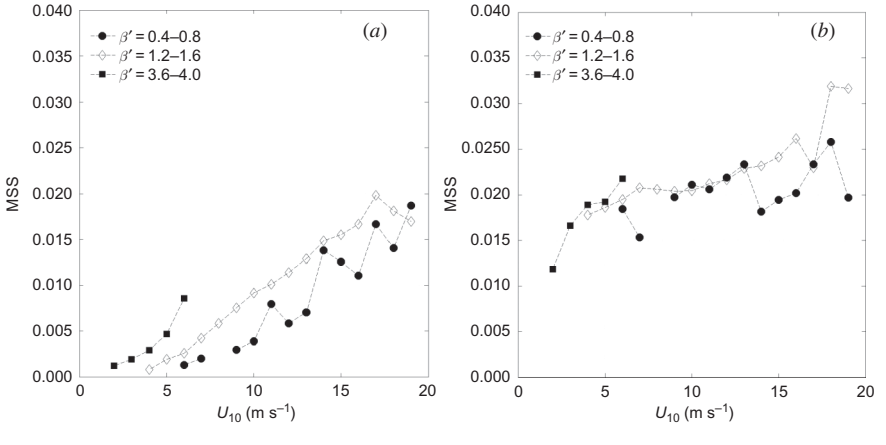

Figure 6. Averaged MSS in U_{10} bins (1 m s^{-1} wide) at different ranges of β' for (*a*) long waves and (*b*) short waves.

5. A spectral model for MSS

As indicated by the preceding discussion, the wave state dependence of the total MSS is mainly ascribed to that of the MSS for long waves, whereas short waves contribute significantly to the magnitude of the total MSS. Thus, it is reasonable to divide the wave spectrum into two parts, which correspond to long gravity waves and short gravity-capillary waves. Equation (7) can be rewritten as

$$s^2 = \int_{k_p}^{k_d} \boldsymbol{k}^2 \left(\varphi_l \left(\vec{\boldsymbol{k}}, U_{10}, \beta \right) + \varphi_h \left(\vec{\boldsymbol{k}}, u_* \right) \right), \tag{9}$$

where $\varphi_l \left(\vec{\boldsymbol{k}}, U_{10}, \beta \right)$ is the wave spectrum for long gravity waves, $\varphi_h \left(\vec{\boldsymbol{k}}, u_* \right)$ is the wave spectrum for short gravity-capillary waves, u_* is the friction velocity of air, $\boldsymbol{k}_p$ is the wave number corresponding to the spectral peak, and $\boldsymbol{k}_d$ is the cut-off wave number. Many investigators have proposed various wave spectra based on measurements or theoretical analysis. The wave spectra proposed by Elfouhaily et al. (1997) are chosen here because they satisfy the 'Plant limit', i.e. an upper limit for the MSS (Plant 2002). In their spectrum for gravity-capillary waves, an equilibrium range parameter, α_m, is included. They proposed two kinds of expressions for it, one is the logarithmic relationship based on the works of Jähne and Riemer (1990) and Hara, Bock, and Lyzenga (1994); the other is the linear relationship consistent with Toba (1973), Kitaigorodskii (1983), and Phillips (1985). In our calculation, u_* is converted into U_{10} using the roughness length z_0 proposed by Donelan et al. (1993) and the logarithmic law for wind speed profile in neutral stabilization conditions:

$$z_0 = 3.7 \times 10^{-5} \left(\frac{U_{10}^2}{g} \right) \left(\frac{U_{10}}{c_p} \right)^{0.9}, \tag{10}$$

$$u_* = \frac{U_{10} \kappa}{\ln (10/z_0)}, \tag{11}$$

where c_p is the phase speed corresponding to the spectral peak of wind waves and $\kappa = 0.4$ is the von Kármán constant. Because the wave spectrum is for the wind waves, the wave age β cannot be greater than 1.2. The calculated MSS with a cut-off wave number of 100 rad m^{-1} (Brown 1990) and the altimeter-measured MSS are shown in Figure 7. The former is more consistent with the latter at low (high) wind speeds by using α_m in the logarithmic (linear) form. In order to improve this limitation, a new relationship for α_m is proposed by combining the logarithmic and linear forms:

$$\alpha_m = 10^{-2} \times \begin{cases} 1.4 + 1.5 \ln \left(\frac{u_*}{c_m} \right) & u_* \le c_m \\ 1.4 \left(\frac{u_*}{c_m} \right) & u_* > c_m \end{cases}, \tag{12}$$

where c_m is the minimum phase speed of gravity capillary waves with a typical value of 0.23 m s^{-1}. It can be seen that the calculated MSS by the modified α_m agrees well with the altimeter MSS in general, at either low or high wind speeds.

Although the calculated MSS and the altimeter MSS are in good agreement, the wave ages β and β' are different in magnitude. The former only indicates the degree of wind wave development, and the latter includes the influence of both wind waves and swells. In order

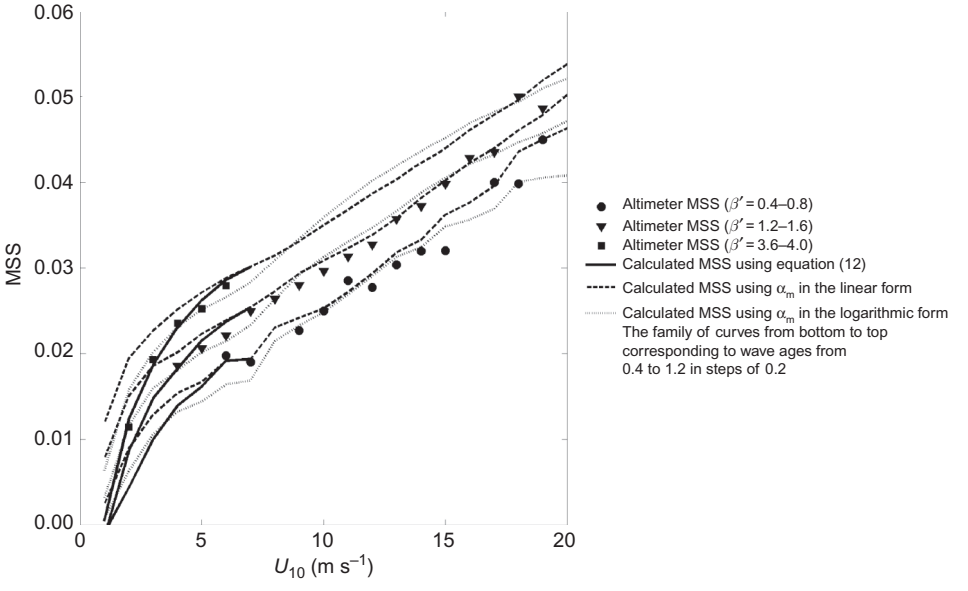

Figure 7. Comparison of the calculated MSS and the altimeter MSS. The symbols correspond to the averaged altimeter MSS within wind speed bins of 1 m s^{-1}.

to directly compare the two kinds of wave age, it is desirable to establish a relationship between them. With the regression analysis, the following relationship is proposed:

$$\beta = \frac{\beta'}{0.5 \times \beta'^{1.15} + 1.2}, \tag{13}$$

With this relationship, a β' value less than 4.0 can be approximately compressed into the range 0.0−1.1, and those values in the range of 4.0−20 are roughly equal to 1.2. After this transition, a good agreement between the calculated MSS and altimeter MSS is obtained at the same wave ages (Figure 8).

6. Application in altimeter wind speed retrieval

Based on Equation (2), Equation (4), and the well-compared calculated MSS proposed above, an NCRS model can be constructed as a function of U_{10} and β. With Equation (13), the wave age β can be obtained from β', which can be calculated from U_{10} and SWH using Equation (6). Thus, the NRCS can be obtained given the value of U_{10} and SWH. With a constant SWH, the NRCS changes with the different wind speeds. The retrieval wind speed is obtained by choosing the one in which the calculated NRCS closely approaches the satellite NRCS.

In order to make the analysis more objective, a new collocated data set is used for validation of the algorithm. The *in situ* data are derived from the same buoys mentioned above, but cover from January 2001 to December 2002. The coincident time and space separation criteria are chosen as 1 h and 50 km, respectively. A total of 914 pairs of data are obtained.

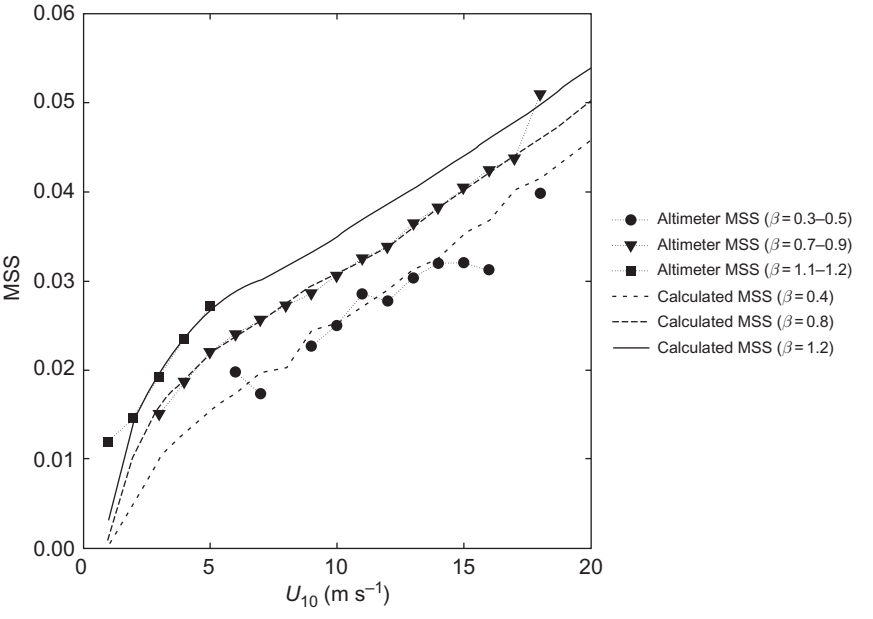

Figure 8. Comparisons of the calculated MSS and altimeter MSS with the converted wave ages. The symbols correspond to the averaged altimeter MSS within wind speed bins of 1 m s^{-1}.

Table 2. Summary of RMSE and bias for various algorithms.

Algorithm	RMSE	Bias
Witter and Chelton (1991)	1.38	−0.11
Lefevre et al. (1994)	2.37	−1.21
Chen et al. (2002)	1.35	−0.09
New algorithm	1.31	0.03

The root mean square error (RMSE) and bias of the wind speed retrieval are listed in Table 2, and RMSEs and biases from three other algorithms are given for comparison. It is clear that the new algorithm yields the best estimation of wind speed compared with other empirical algorithms in terms of both RMSEs and biases.

7. Summary

Instead of being considered as a constant, the reflection coefficient is proposed as a function of wind speed, which is then used to determine the MSS by the T/P NRCS of Ku-band. It is shown that the MSS increases with the wave age, which is mainly ascribed to the effect of wind waves. The MSS increases with the increasing SWH corresponding to wind waves and is independent of the SWH of swell. The wave effect is mainly due to the contribution of the longer waves rather than the shorter waves.

Based on the spectrum proposed by Elfouhaily et al. (1997), a spectral model for MSS is proposed, which depends on wind speed and SWH. The calculated MSS agrees well with the altimeter MSS when the pseudo-wave is adjusted to describe the development of wind waves. This spectral model is utilized to derive wind speeds from the NRCS and SWH of

T/P. Compared with previous empirical algorithms, the new algorithm performs better in terms of both RMSE and bias.

Acknowledgements

The authors are grateful to Ms Katie Costa for the English proofreading. TOPEX altimeter and buoy data are provided by the NASA TOPEX/POSEIDON Project and the National Data Buoy Center. This work is supported by the National Basic Research Programme of China (2009CB421200) and the National Natural Science Foundation of China (41076007, 4093044). This work is also funded by the OUC 111 project and Innovation and Research Foundation of Ocean University of China.

References

Apel, J. R. 1994. "An Improved Model of the Ocean Surface Wave Vector Spectrum and Its Effects on Radar Backscatter." *Journal of Geophysical Research* 99, no. C8: 16269–91.

Barrick, D. 1974. "Wind Dependence of Quasi-Specular Microwave Sea Scatter." *IEEE Transactions on Antennas and Propagation* 22, no. 1: 135–6.

Brown, G. S. 1990. "Quasi-Specular Scattering from Air–Sea Interface." In *Surface Waves and Fluxes*, edited by G. Geerneart, and W. Plant, 1–40. New York: Springer.

Chen, G., B. Chapron, R. Ezraty, and D. Vandemark. 2002. "A Dual-Frequency Approach for Retrieving Sea Surface Wind Speed from TOPEX Altimetry." *Journal of Geophysical Research* 107, no. C12: 3226–35.

Cheng, Y., Q. Xu, Y. Liu, H. Lin, P. Xiu, X. Yin, H. Zong, and Z. Rong. 2008. "An Analytical Algorithm with a Wave Age Factor for Altimeter Wind Speed Retrieval." *International Journal of Remote Sensing* 29, no. 19: 5699–716.

Cox, C., and W. Munk. 1954. "Statistics of the Sea Surface Derived from Sun Glitter." *Journal of Marine Research* 13, 198–227.

Donelan, M. A., F. W. Dobson, S. D. Smith, and R. J. Anderson. 1993. "On the Dependence of Sea Surface Roughness on Wave Development." *Journal of Physical Oceanography* 23, no. 9: 2143–9.

Earle, M. D. 1984. *Development of Algorithms for Separation of Sea and Swell*. National Data Buoy Center Technical Report No. MEC-87-1, National Data Buoy Center, Stennis Space Center, MS, 53.

Elfouhaily, T., B. Chapron, K. Katsaros, and D. Vandemark. 1997. "A Unified Directional Spectrum for Long and Short Wind-Driven Waves." *Journal of Geophysical Research* 102, no. C7: 15781–96.

Freilich, M. H., and B. A. Vanhoff. 2003. "The Relationship between Winds, Surface Roughness, and Radar Backscatter at Low Incidence Angles from TRMM Precipitation Radar Measurements." *Journal of Atmosphere and Oceanic Technology* 20, no. 4: 549–62.

Frew, N. M., D. M. Glover, E. J. Bock, and S. J. Mccue. 2007. "A New Approach to Estimation of Global Air–Sea Gas Transfer Velocity Fields Using Dual-Frequency Altimeter Backscatter," *Journal of Geophysical Research* 112, C11003. doi:10.1029/2006JC003819.

Glazman, R. E., and A. Greysukh. 1993. "Satellite Altimeter Measurements of Surface Wind." *Journal of Geophysical Research* 98, no. C2: 2475–83.

Glazman, R. E., and S. H. Pilorz. 1990. "Effects of Sea Maturity on Satellite Altimeter Measurements." *Journal of Geophysical Research* 95, no. C3: 2857–70.

Gourrion, J., D. Vandemark, S. Bailey, B. Chapron, G. P. Gommenginger, P. G. Challenor, and M. A. Srokosz. 2002. "A Two-Parameter Wind Speed Algorithm for Ku-Band Altimeters." *Journal of Atmosphere and Oceanic Technology* 19, no. 12: 2030–48.

Hara, T., E. J. Bock, and D. Lyzenga. 1994. "*In Situ* Measurements of Capillary-Gravity Wave Spectra Using a Scanning Laser Slope Gauge and Microwave Radars." *Journal of Geophysical Research* 99, no. C6: 12593–602.

Hauser, D., G. Caudal, S. Guimbard, and A. Mouche. 2009. "Reply to Comment by Paul A. Hwang on 'a Study of the Slope Probability Density Function of the Ocean Waves from Radar Observations" by D. Hauser et al.' *Journal of Geophysical Research* 114, no. C2: C02009. doi:10.1029/2008JC005117.

Holliday, D., G. St-Cyr, and N. E. Woods. 1986. "A Radar Ocean Imaging Model for Small to Moderate Incidence Angles." *International Journal of Remote Sensing* 7, no. 12: 1809–34.

Jackson, F. C., W. T. Walton, D. E. Hines, B. A. Walter, and C. Y. Peng. 1992. "Sea Surface Mean Square Slope from Ku-Band Backscatter Data." *Journal of Geophysical Research* 97, no. C7: 11411–27.

Jähne, B., and K. S. Riemer. 1990. "Two-Dimensional Wave Number Spectra of Small-Scale Water Surface Waves." *Journal of Geophysical Research* 95, no. C7: 11531–46.

Kitaigorodskii, S. A. 1983. "On the Theory of the Equilibrium Range in the Spectrum of Wind-Generated Gravity Waves." *Journal of Physical Oceanography* 13, no. 5: 816–27.

Lefevre, J. M., J. Barckicke, and Y. Ménard. 1994. "A Significant Wave Height Dependent Function for TOPEX/POSEIDON Wind Speed Retrieval." *Journal of Geophysical Research* 99, no. C12: 25035–49.

Nghiem, S. V., F. K. Li, S. Lou, G. Neumann, R. E. Mcintosh, S. C. Carson, J. R. Carswell, E. J. Walsh, M. A. Donelan, and W. M. Drennan. 1995. "Observations of Radar Backscatter at Ku and C Bands in the Presence of Large Waves during the Surface Wave Dynamics Experiment." *IEEE Transactions on Geoscience and Remote Sensing* 33, no. 3: 708–21.

Phillips, O. M., ed. 1977. *The Dynamics of the Upper Ocean*. 2nd ed., 336. Cambridge: Cambridge University Press.

Phillips, O. M. 1985. "Spectral and Statistical Properties of the Equilibrium Range in Wind-Generated Gravity Waves." *Journal of Fluid Mechanics* 156, no. 1: 505–31.

Plant, W. J. 2002. "A Stochastic, Multiscale Model of Microwave Backscatter from the Ocean." *Journal of Geophysical Research* 107, no. C9: 3120. doi:10.1029/2001JC000909.

Toba, Y. 1973. "Local Balance in the Air–Sea Boundary Processes. III. On the Spectrum of Wind Waves." *Journal of Oceanography* 29, 209–25.

Tran, N., O. Z. Zanife, B. Chapron, D. Vandemark, and P. Vincent. 2005. "Absolute Calibration of Jason-1 and Envisat Altimeter Ku-Band Radar Cross Sections from Cross Comparison with TRMM Precipitation Radar Measurements." *Journal of Atmosphere and Oceanic Technology* 22, no. 9: 1389–402.

Valenzuela, G. R. 1978. "Theories for the Interaction of Electromagnetic and Oceanic Waves – A Review." *Boundary-Layer Meteorology* 13, no. 1: 61–85.

Vandemark, D., B. Chapron, J. Sun, G. H. Crescenti, and H. C. Graber. 2004. "Ocean Wave Slope Observations Using Radar Backscatter and Laser Altimeters." *Journal of Physical Oceanography* 34, no. 12: 2825–42.

Walsh, E. J., D. C. Vandemark, C. A. Friehe, S. P. Burns, D. Khelif, R. N. Swift, and J. F. Scott. 1998. "Measuring Sea Surface Mean Square Slope with a 36-GHz Scanning Radar Altimeter." *Journal of Geophysical Research* 103, no. C6: 12587–601.

Witter, D. L., and D. B. Chelton. 1991. "A Geosat Altimeter Wind Speed Algorithm and a Method for Altimeter Wind Speed Algorithm Development." *Journal of Geophysical Research* 96, no. C5: 8853–60.

Wu, J. 1988. "Wind-Stress Coefficients at Light Winds." *Journal of Atmosphere and Oceanic Technology* 5, no. 6: 885–8.

Wu, J. 1992. "Near-Nadir Microwave Specular Returns from the Sea Surface – Altimeter Algorithms for Wind and Wind Stress." *Journal of Atmosphere and Oceanic Technology* 9, no. 5: 659–67.

Wu, J. 1990. "Mean Square Slopes of the Wind-Disturbed Water Surface, Their Magnitude, Directionality, and Composition." *Radio Science* 25, no. 1: 37–48.

Zhao, D., and Y. Toba. 2003. "A Spectral Approach for Determining Altimeter Wind Speed Model Functions." *Journal of Oceanography* 59, no. 2: 235–44.

Zheng, Q. A., V. Klemas, G. S. Hayne, and N. E. Huang. 1983. "The Effect of Oceanic Whitecaps and Foams on Pulse-Limited Radar Altimeters." *Journal of Geophysical Research* 88, no. C4: 2571–8.